Journal of Magnetism and Magnetic Materials 417 (2016) 69–74

Contents lists available at ScienceDirect

Journal of Magnetism and Magnetic Materials

journal homepage: www.elsevier.com/locate/jmmm

Pressure induced insulator–metal transition and giant negative piezoresistance in $Pr_{0.6}Ca_{0.4}Mn_{0.96}Al_{0.04}O_3$ polycrystal

S. Arumugam [a,*], R. Thiyagarajan [b], G. Kalaiselvan [a], P. Sivaprakash [a]

[a] Centre for High Pressure Research, School of Physics, Bharathidasan University, Tiruchirapalli 620024, Tamil Nadu, India
[b] Center for High Pressure Science and Technology Advanced Research (HPSTAR), Shanghai 201203, People's Republic of China

ARTICLE INFO

Article history:
Received 22 February 2016
Received in revised form
16 May 2016
Accepted 20 May 2016
Available online 21 May 2016

Keywords:
High pressure
Charge-orbital-insulating manganites
Insulator–metal transition
Piezoresistance

ABSTRACT

The effect of external hydrostatic pressure (P) on the magnetization (M) and resistivity (ρ) properties of charge-orbital (CO) ordered-insulating phase-separated manganite $Pr_{0.6}Ca_{0.4}Mn_{0.96}Al_{0.04}O_3$ system is reported here. At ambient P, CO ordering transition and spin-canting in the AFM are observed at 223 K and 55 K respectively in $M(T)$ and $\rho(T)$ measurements. Application of P increases simultaneously the magnitude of magnetization (M) and transition temperature, and weakens the CO ordering in $M(T)$ measurements up to 0.98 GPa. During $\rho(T)$ measurements, P induces an insulator–metallic transition (T_{IM}) at 1.02 GPa, and further increase of P up to 2.84 GPa leads to increase of T_{IM} ($dT_{IM}/dP = 21.6$ K/GPa). ρ at T_{IM} is reduced about three orders of magnitude at 2.84 GPa, and leads to the giant negative piezoresistance (~98%). These results are analyzed separately in two temperature regions *i.e.*, below and above T_{IM} by power function equation and small polaronic hopping model respectively. It is understood from these analyses that the application of P suppresses the Jahn–Teller distortions, electron–electron and electron–magnon scattering factors, and induces the insulator–metal transition in $Pr_{0.6}Ca_{0.4}Mn_{0.96}Al_{0.04}O_3$ system.

1. Introduction

Perovskite manganites $Ln_{1-x}A_xMnO_3$ (Ln:La or rare-earth elements; A:alkaline metals) have been extensively studied for more than two decades, because of their rich physics and their potential applications due to the interesting properties such as colossal magnetoresistance (CMR), charge-orbital (CO) ordering, Jahn–Teller (JT) effect and Double-Exchange (DE) mechanism etc [1]. These materials get a great deal of attraction by having the ferromagnetic (FM)-paramagnetic (PM) transition accompanied by insulator–metal (IM) transition, which is originating from the DE interaction [2]. It is widely accepted that DE mechanism [3] and hopping of small polarons [4] are responsible for the ferromagnetic metallic (FMM) and paramagnetic insulating (PMI) states of manganites respectively. On the other hand, both magnetic and transport properties of manganites are controlled by the bandwidth and band filling, and these can be altered through internal (chemical) pressure by doping at the Ln, A or Mn site, and/or external perturbations such as magnetic field (H), uniaxial pressure (UP) and hydrostatic pressure (P). In particular, numerous studies of pressure effect on various manganites revealed an increase of the transition temperature with P [5]. P enhances hopping integral t_0 by affecting the orbital degeneracy without altering total spin of the system, and consequently changes the Curie temperature (T_C) as well as IM temperature (T_{IM}).

Generally, the change of resistivity by H and P is coined by terms Magnetoresistance (MR) and piezoresistance (PR) respectively, and they have been classified into normal, giant and colossal depending upon the order of change in resistance. The study on MR has been largely discussed in various perovskite and bilayer manganite systems; however, PR has been studied less comparatively. Previously, Zhang et al. [6] and Mohan Radheep et al. [7] reported the giant and colossal PR in $La_{0.85}Sr_{0.15}MnO_3$ and $Sm_{0.55}(Sr_{0.5}Ca_{0.5})_{0.45}MnO_3$ by the application of UP of 30 MPa and 90 MPa respectively.

In $Pr_{1-x}Ca_xMnO_3$ manganite system, the large size difference between the Pr/Ca and the Mn cations leads to a small tolerance factor, and small transfer integral between Mn atoms [8]. Hence, the e_g electrons are localized and the charge-ordering (CO) phase is stabilized in a broad doping range $0.3 \le x \le 0.7$, and antiferromagnetic insulator (AFI) at low temperatures. However, the internal and external perturbations can destroy the CO state, and lead to a conducting state. *i.e.*, insulating nature of CO ordered manganites was destroyed internally by doping at Ln, A- [9] and/or Mn-sites [10–12], externally by magnetic field [13] and/or pressure [14]. For example, neutron diffraction studies under pressure upto

* Corresponding author.
E-mail address: sarumugam1963@yahoo.com (S. Arumugam).

http://dx.doi.org/10.1016/j.jmmm.2016.05.065
0304-8853/

2.3 GPa on $Pr_{0.75}Na_{0.25}MnO_3$ system reveals the suppression of the CE-type AFM CO state. Similarly, CO ordered state on $Pr_{1-x}Ca_xMnO_3$ was also suppressed by the effect of the internal [15] and external perturbations [16–18]. Tomioka et al. reported the suppression of CO ordered insulator and induces the FMM transition by Sr doping at A site of $Pr_{0.7}Ca_{0.3}MnO_3$ *i.e.*, $Pr_{0.55}(Ca_{1-y}Sr_{1-y})_{0.45}MnO_3$ ($y > 0.25$) [15], and application of $H > 2$ T also leads to similar phenomenon [16]. Similarly, Suresh Kumar et al. has also reported the IM transition in $Pr_{0.6}Ca_{0.4}MnO_3$ with the Mn-site doping by various impurities such as Cr, Co, Ni and Ru at ambient P [17]. However, Al doping at Mn site *viz.*, $Pr_{0.6}Ca_{0.4}Mn_{0.96}Al_{0.04}O_3$ does not exhibit IM transition, but only weak CO ordering was reported at low temperature [17]. On the other hand, P suppressed CO ordered insulating state in $Pr_{1-x}Ca_xMnO_3$ system at 3.8 GPa, 2.8 GPa and 2.0 GPa for $x=0.25$, 0.3 and 0.35 respectively, and correspondingly induced IM transition [18,19]. Hence, P may destabilize the CO state in $Pr_{0.6}Ca_{0.4}Mn_{0.96}Al_{0.04}O_3$ system. By keeping these points in mind, we have selected $Pr_{0.6}Ca_{0.4}Mn_{0.96}Al_{0.04}O_3$ system to investigate the effect of P on magnetization, resistivity and order of phase transition in a more detailed way.

2. Experimental

Polycrystalline samples of $Pr_{0.6}Ca_{0.4}Mn_{0.96}Al_{0.04}O_3$ were prepared using the standard solid-state reaction method. Further, details of sample preparation, structural characterization, magnetization and transport properties at ambient P were reported by Suresh Kumar et al. [17]. Magnetic measurements at various P up to ~1 GPa were performed using Physical Property Measurement System-Vibrating Sample Magnetometer (PPMS-VSM), (Quantum Design, USA) module equipped with the Cu–Be clamp type pressure cell. The temperature dependence of magnetization [$M(T)$] was recorded upon cooling and warming cycles with an applied magnetic field of $\mu_0 \cdot H = 0.1$ T in the temperature range of 300–2 K at various P. The magnetic transition temperature was determined from the inflection point of dM/dT curve. Magnetization as a function of magnetic field [$M(H)$] was recorded during increasing and decreasing magnetic field ($\mu_0 \cdot H$) between 0 and 5 T at various P with a temperature interval of 10 K. The pressure dependence of T_C of superconducting Sn was used as an *in-situ* pressure standard for calculating the actual pressure experienced by the sample in the pressure cell [20]. The temperature dependence of electrical resistivity [$\rho(T)$] under ambient and various P was measured by a conventional four-probe method for cooling and warming cycles using closed cycle refrigerator – variable temperature insert (CCR-VTI, Sumitomo, Japan) and 3 GPa self clamp-type hybrid hydrostatic pressure cell. The pressure was calibrated using resistive transitions of Bi I–II (2.55 GPa) and Bi II–III (2.7 GPa) at room temperature [21].

3. Results and discussion

3.1. Effect of pressure on magnetic measurements

Fig. 1(a) shows the $M(T)$ of $Pr_{0.6}Ca_{0.4}Mn_{0.96}Al_{0.04}O_3$ at ambient P under the magnetic field ($\mu_0 \cdot H$) of 0.1 T. A weak maximum around 223 K (T_{CO}) [shown in inset] is observed and it is a hall mark of the CO ordering transition. The peak at 55 K (95 K) during the cooling (warming) cycle corresponds to the spin-canting in the AFM state of Mn sublattice, and these results are in good agreement with Suresh Kumar et al. [17]. The thermal hysteresis around spin-canting transition between cooling and warning cycles suggests a first-order transition in nature [22]. Further, Fig. 1(a) shows a weak

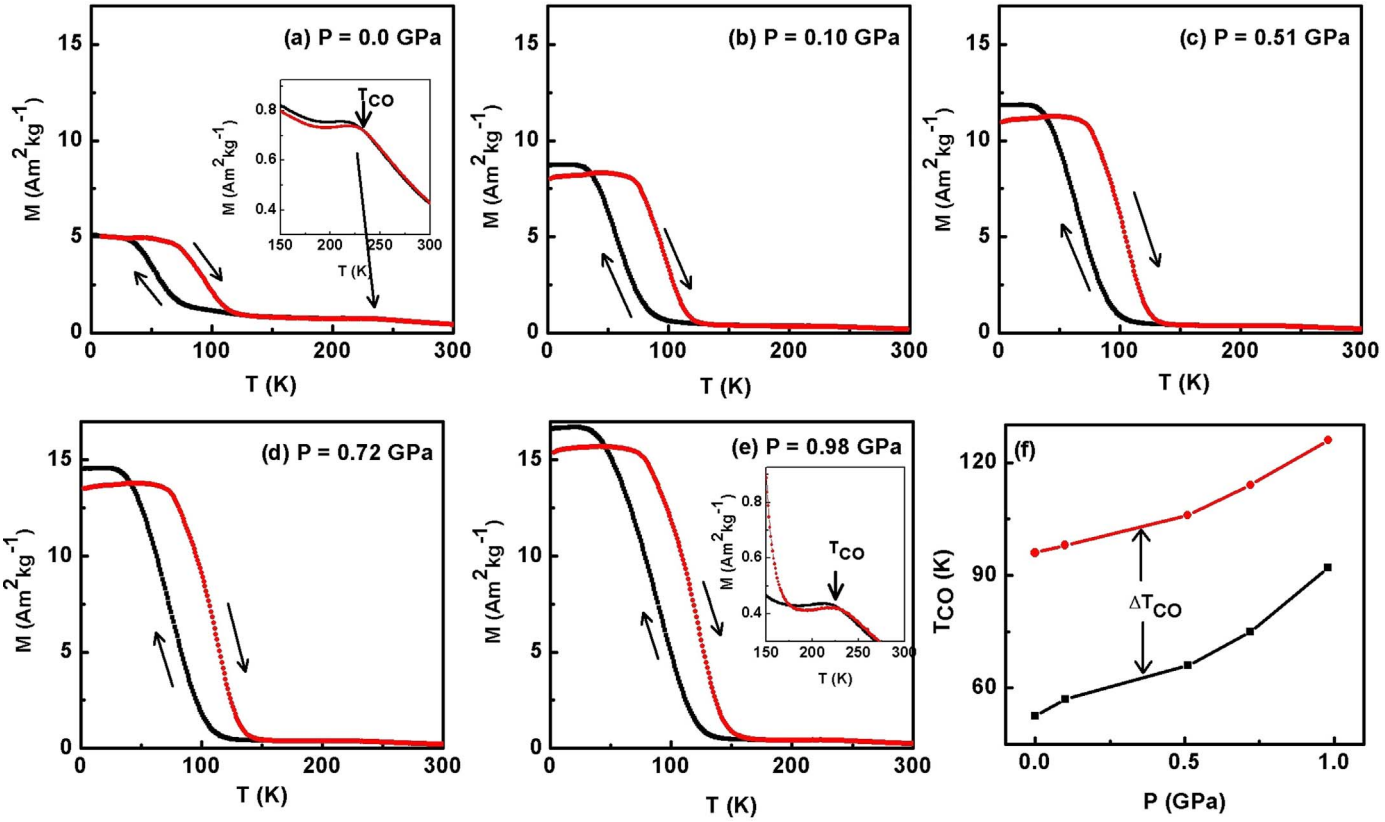

Fig. 1. Temperature dependence of magnetization for $Pr_{0.6}Ca_{0.4}Mn_{0.96}Al_{0.04}O_3$ at hydrostatic pressure of (a) 0 [Inset: enlarged view around CO ordering transition], (b) 0.10, (c) 0.51, (d) 0.72 and (e) 0.98 GPa; (f) pressure dependence of T_T during cooling and warming cycles.

magnitude for magnetization, and indicates that the doping of Al at Mn site do not alter the CO ordered state of parent compound $Pr_{0.6}Ca_{0.4}MnO_3$. Martin et al. also confirms the presence of CO ordering and spin-canting in the AFM state at ~220 K and 50 K respectively in $Pr_{0.5}Ca_{0.5}Mn_{0.95}Al_{0.05}O_3$ [23]. Fig. 1(b)–(e) shows that $M(T)$ of $Pr_{0.6}Ca_{0.4}Mn_{0.96}Al_{0.04}O_3$ under $\mu_0 \cdot H$ of 0.1 T at P=0.10, 0.51, 0.72 and 0.98 GPa respectively. It is clear from these figures that the application of P from 0 to 0.98 GPa increases the magnitude of magnetization from 5 A m^2 kg^{-1} [Fig. 1(b)] to 15 A m^2 kg^{-1} [Fig. 1(e)] at low temperatures, and also shifts the transition temperature towards high-temperature region. Inset of Fig. 1(e) shows that the enlarged view of $M(T)$ around CO transition at 0.98 GPa. It is understood from these results that P of 0.98 GPa is not enough to suppress both CO ordered state and first-order transition completely. Fig. 1(f) shows the P dependence of T_{CO} for $Pr_{0.6}Ca_{0.4}Mn_{0.96}Al_{0.04}O_3$ sample. The rate of change of T_{CO} with respect to P (dT_{CO}/dP) is found to be 37 K/GPa, and it is same for both cooling and warming cycles. Hence, it confirms that the $Pr_{0.6}Ca_{0.4}Mn_{0.96}Al_{0.04}O_3$ system retains a first-order transition by the application of P up to 0.98 GPa.

We have measured $M(H)$ curves from 30 to 130 K in every 10 K interval at various P such as 0 GPa, 0.51 GPa, 0.72 GPa and 0.98 GPa, as shown in Fig. 2(a)–(d) respectively. The sample was zero-field cooled from 250 K to the 30 K prior to the measurement to erase previous magnetic memory. At ambient P, $M(H)$ at 30 K increases rapidly up to 3 T and then follows by moderate increase and saturates at 5 T. This saturation is due to the progressive conversion of the CO ordered matrix into a FM phase. When H is reduced from 5 T, the magnetization traces a separate S-type path due to the field-induced metamagnetic transition (FIMMT) with the first-order nature. $M(H)$ curves from 30 K to 100 K shows that both magnetization and S-type behavior decreases with increasing of H up to 5 T. Further, $M(H)$ curves above 110 K increase linearly up to 5 T corresponds to the CO ordering transition. From the Fig. 2 (b)–(d), it is observed that the application of P up to 0.98 GPa reduces slightly both S-type behavior and width of the hysteresis. Moreover, the value of saturated magnetization (M_S) at ambient P is 3.64 μ_B/Mn at T=30 K and H=5 T. Application of P up to 0.72 GPa reduces M_S to 3.4 μ_B/Mn, and further increase of P upto 0.98 GPa reduces to 3.14 μ_B/Mn at T=30 K (*i.e.,* below transition) and H=5 T. However, there is no appreciable change in M_S by application of P up to 0.98 GPa at T=130 K (*i.e.,* above transition) and H=5 T. It is confirmed that 1 GPa is not enough for the complete suppression of CO ordering, FIMMT and first-order behavior in this system. It was not possible to possible magnetization measurements for the pressure more than 1 GPa due to limitation of our pressure cell used for magnetization measurements. Hence, we have carried out $\rho(T)$ measurements under various P up to ~3 GPa in order to study the effect of P in detail.

3.2. Effect of pressure on resistivity measurements

Fig. 3(a) shows the $\rho(T)$ of $Pr_{0.6}Ca_{0.4}Mn_{0.96}Al_{0.04}O_3$ sample for various P up to 2.84 GPa during the warming cycle. At ambient P, the sample shows sharp rise in resistivity below 200 K which manifests to CO insulting nature. Further, it exhibits insulating nature with a short "*shoulder*"-like transition around 100 K, which is analogous to the spin-canting transition of magnetization measurements. These transitions are also in good agreement with the results reported by Suresh Kumar et al. [17]. The application of P of 0.43 GPa does not change the insulating behavior in the high-temperature region, whereas it reduces the magnitude of resistivity in the low-temperature semiconducting region. Further, increase of P upto 1.02 GPa induces IM transition (T_{IM}) at 107 K [Fig. 3(a)], and an enlarged view around the transition region is shown as an inset of Fig. 3(a). Further increase in P up to 2.84 GPa enhances metallic nature of the sample, and shifts T_{IM} towards higher temperature. The P dependence of T_{IM} is shown in the left

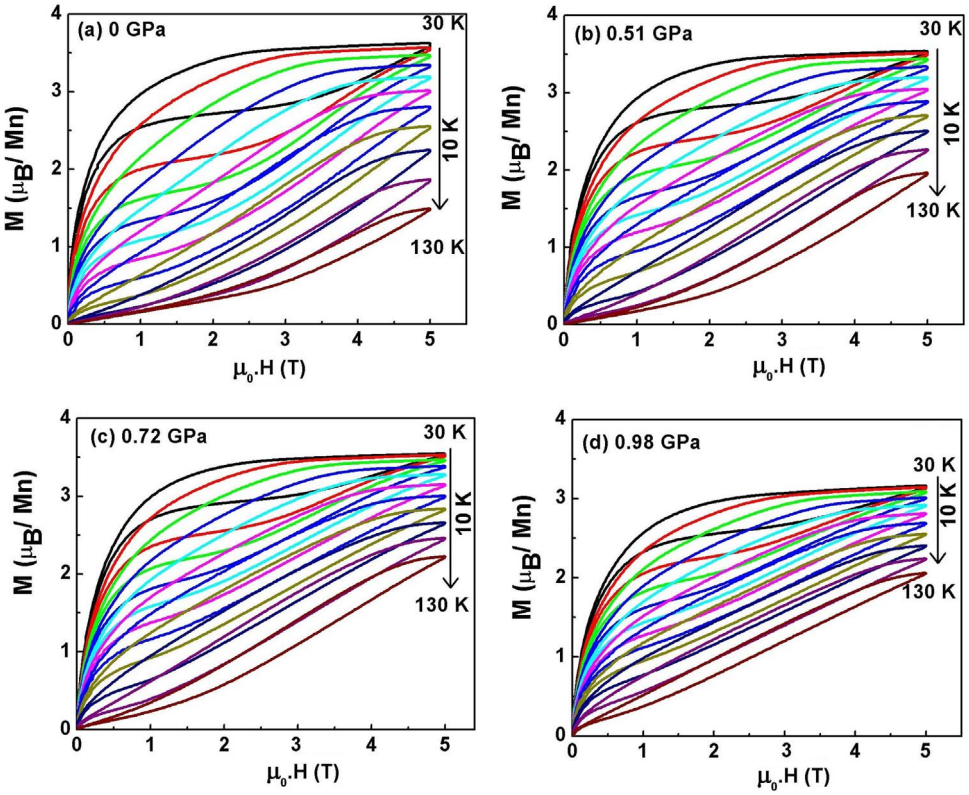

Fig. 2. Magnetic field dependence of magnetization for $Pr_{0.6}Ca_{0.4}Mn_{0.96}Al_{0.04}O_3$ at hydrostatic pressure of (a) 0, (b) 0.51, (c) 0.72 and (d) 0.98 GPa for various temperatures around transition in the step of 10 K.

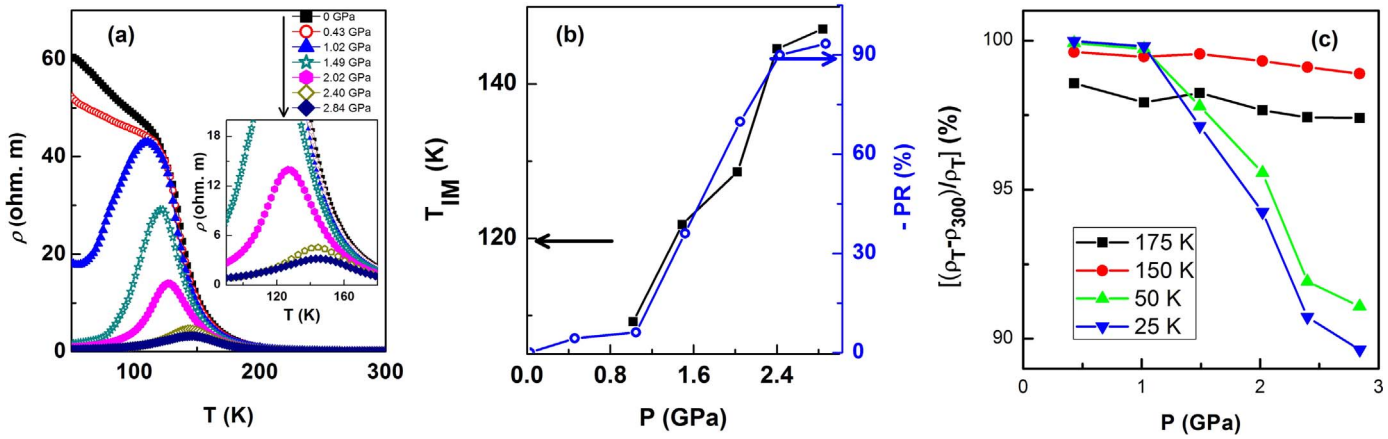

Fig. 3. (a) Temperature dependence of resistivity for $Pr_{0.6}Ca_{0.4}Mn_{0.96}Al_{0.04}O_3$ under various hydrostatic pressure up to 2.84 GPa during the warming cycle [Inset: enlarge view of main graph]; (b) pressure dependence of T_{IM} (left axis) and Piezoresistance (right axis); (c) loss percentage of normalized resistivity at 25 K, 50 K, 150 K and 175 K.

axis of Fig. 3(b), and the rate of change of T_{IM} with respect to P [dT_{IM}/dP] is found to be 21.6 K/GPa.

The change in magnitude of resistivity by P at transition temperature is analyzed by estimating the Piezoresistance (PR) for various P up to 2.84 GPa using the following relation: $-\mathrm{PR}=\{([\rho(P)-\rho(0)])/\rho(0)\}\times 100\%$. The P dependence of -PR is shown in the right axis of Fig. 3(b). Initially, -PR slowly increases up to 1.02 GPa, and found to increase drastically between 1.02 to 2.40 GPa. The maximum $-$PR of 98% is observed at T_{IM} for $P=2.84$ GPa. Thus, $Pr_{0.6}Ca_{0.4}Mn_{0.96}Al_{0.04}O_3$ exhibits Giant negative Piezoresistance under P of 2.84 GPa.

The P dependence ρ below and above T_{IM} is analyzed by the *loss percentage of normalized resistivity*. It is calculated from the change in resistivity for T (150 K, 175 K) $> T_{IM}$ and T (50 K, 25 K) $< T_{IM}$ and room temperature resistivity, and using the relation $\{([\rho_T-\rho_{300}])/\rho_T\}\times 100\%$. The pressure dependence of loss percentage of normalized resistivity is shown in Fig. 3(c) and it is found that there is no appreciable change in loss percentage of normalized resistivity with the increase of P above T_{IM}. However, loss percentage of normalized resistivity of 9% and 11% are observed at 50 and 25 K respectively, and indicates switching-like behavior by the application of P.

4. Discussion

Al^{3+} substitution to the Mn site of $Pr_{0.6}Ca_{0.4}MnO_3$ (*viz.*, $Pr_{0.6}Ca_{0.4}Mn_{0.96}Al_{0.04}O_3$) is isoelectronic to Mn^{4+} (t_{2g}^3) ion, the number of Jahn–Teller active Mn^{3+} ions are getting reduced. Hence, it leads to the weakening of CO state slightly, but does not make the sample completely to FM state at ambient P condition [17]. Generally, application of P in manganites decreases the Mn–O bond length and increases Mn–O–Mn bond angle towards 180°, hence enhances both the charge transfer process and conduction (e_g electron) bandwidth. Thus, the external P diminishes the Super Exchange interactions, so CO ordering state getting melted. At the same time, it favors the DE interaction, and the FM metallic phase is stabilized subsequently. Thus, the prototypical narrow band manganite $Pr_{0.65}Ca_{0.35}MnO_3$ also shows the transition from CO insulating state to FMM state by the application of $P=2.0$ GPa [18]. However, the required amount of P to destabilize CO ordering state is found to be reduced by half (*i.e.*, 1 GPa) in $Pr_{0.6}Ca_{0.4}Mn_{0.96}Al_{0.04}O_3$ system compared to $Pr_{0.65}Ca_{0.35}MnO_3$ sample, and it is due to simultaneous effect of internal (doping) and external (hydrostatic pressure) perturbations. In order to understand the nature of the conduction mechanism under various P, it would be better to analyze and discuss in two different temperature regions separately such as: (i) melting of CO ordering in the insulting phase above T_{IM} and (ii) spin-canting semiconducting state to FMM phase below T_{IM}, as follows:

4.1. Melting of CO ordering state by pressure in the high-temperature region

Since high-temperature polaronic phase depends on the activation energy (E_a) of the system, we have determined E_a from $\rho(T)$ in the high-temperature ($T_{IM} < T$) region under various P using small polaronic hopping model [24]

$$\rho(T) = \rho_\alpha T \exp(E_a/k_B T)$$

where ρ_α and E_a are the residual resistivity and activation energy of polaron hopping conduction respectively. From the slopes of ln (ρ/T) *vs* ($1/T$) plot, E_a is calculated in the high-temperature region for various P using the above equation, and the values are shown in Table 1. The value of $E_a=113$ meV at 0 GPa, and it is approximately closer to the values reported for perovskite manganites. There is no appreciable change in E_a is observed below 1 GPa. However, as P increases above 1 GPa, E_a decreases monotonically upto 2.84 GPa. High-temperature polaronic phase is generally believed due to Jahn–Teller distortion that splits the two e_g orbitals. The hole doping by Al^{3+} weakens the Jahn–Teller distortion and high-temperature polaronic state. In addition to this effect, the application of P closes the gap in e_g orbitals and reduces the activation energy. This phenomenon melts the CO ordering nature of Al^{3+} doped sample in the high-temperature region. Similar effect has been observed in the high temperature region for various manganite systems [25–27].

Table 1
Values of the coefficients obtained by fitting of $\rho(T)$ data in power functions (below T_{IM}) and the small polaronic hopping model (above T_{IM}).

P (GPa)	Below T_{IM}		Above T_{IM}
	ρ_2 (Ω cm K^{-2})	$\rho_{4.5}\times 10^{-8}$ (Ω cm K$^{-4.5}$)	Activation energy E_a (meV)
0.00	–	–	113.41
0.43	–	–	112.33
1.02	0.589	148.78	110.07
1.49	0.245	40.48	106.58
2.02	0.095	26.15	104.53
2.40	0.017	5.74	103.79
2.84	0.018	0.79	100.90

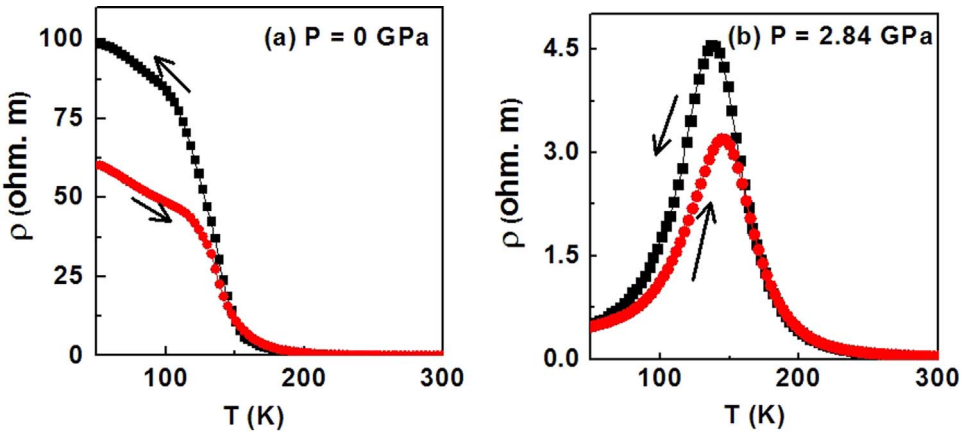

Fig. 4. Temperature dependence of resistivity of $Pr_{0.6}Ca_{0.4}Mn_{0.96}Al_{0.04}O_3$ during cooling and warming cycles under hydrostatic pressure of (a) 0 GPa and (b) 2.84 GPa.

4.2. Pressure-induced insulator–metallic transition in low-temperature region

As shown in Fig. 3(a), $\rho(T)$ of $Pr_{0.6}Ca_{0.4}Mn_{0.96}Al_{0.04}O_3$ exhibits IM transition for $P > 1.02$ GPa. In the low-temperature region, metallic phase is approximated by an expression that includes some scattering mechanisms: $\rho(T) = \rho_0 + \rho_2 T^2 + \rho_{4.5} T^{4.5}$, where ρ_0 is the temperature-independent residual resistivity, the term $\rho_2 T^2$ describes the resistivity associated with mutual scattering of charge carriers, and $\rho_{4.5} T^{4.5}$ associated with electron–magnon scattering processes [28]. The other scattering mechanisms caused by one-magnon ($\rho_3 T^3$) and electron-phonon ($\rho_5 T^5$) interactions at low temperatures did not fitted well [29]. Hence, our results are better described by this equation. The values of the coefficients such as ρ_0, ρ_2 and $\rho_{4.5}$ in the low-temperature region are estimated by fitting the $\rho(T)$ data to the above equation for various P above 1.02 GPa, and the corresponding values are given in Table 1. Since the above equation is valid only for the metallic ground state, it is not possible to estimate the coefficients for the set data $P=0$ and 0.43 GPa. It is inferred that the values of ρ_2 and $\rho_{4.5}$ are decreased by the application of *P. i.e., P* reduces the scattering of charge carriers and electron–magnon scattering. Hence, reduction of scattering in the low-temperature region enhances electron transfer integral between $3d_{x^2-y^2}$ and $3d_{z^2-r^2}$ states through DE phenomenon. As a consequence, ρ in the spin-canting region is reduced much by the application of P and leads to the metallic state in $Pr_{0.6}Ca_{0.4}Mn_{0.96}Al_{0.04}O_3$ system.

4.3. Effect of P on order of transition

Effect of P on the order of phase transition in the resistivity measurements for $Pr_{0.6}Ca_{0.4}Mn_{0.96}Al_{0.04}O_3$ is also studied. Fig. 4 (a) and (b) show the $\rho(T)$ of $Pr_{0.6}Ca_{0.4}Mn_{0.96}Al_{0.04}O_3$ during cooling and warming cycles at 0 GPa and 2.84 GPa respectively. As discussed above, $M(T)$ exhibits hysteresis around transition at ambient P, and the hysteresis is retained by the application of P up to 0.98 GPa. $\rho(T)$ plots at 0 GPa shows hysteresis between cooling and warming cycles around insulator to semiconducting transition. Further, application of P up to 2.84 GPa do not show any appreciable changes in the width of the hysteresis [Fig. 4(b)]. Hence, it is confirmed that P of 2.84 GPa is not enough to change the first- to second-order transition and very high P is may be required for the suppression of the first-order transition in this sample.

Generally, the first-order transition is always accompanied by a structural change, and hence this CO insulating to metallic transition is the structural transition in nature [14]. Nevertheless, the external P changes the properties of the systems mainly through changes in lattice parameters. The earlier studies of the pressure dependent neutron diffraction measurements on similar systems confirmed the orthorhombic to cubic structural phase transition [30]. In the present work, structural transition is retained by keeping first-order nature even under P up to 2.84 GPa for the $Pr_{0.6}Ca_{0.4}Mn_{0.96}Al_{0.04}O_3$ sample. Thus, coexistence of the giant negative PR with structural phase transition leads to a *switching-like* behavior [Fig. 3(c)].

5. Conclusion

In summary, we have measured the effect of hydrostatic pressure on magnetization and transport properties of $Pr_{0.6}Ca_{0.4}Mn_{0.96}Al_{0.04}O_3$ sample. As P increase of P, low-temperature scattering factors and high-temperature activation energy significantly decreases monotonically. This behavior suppresses the formation of polaronic state in the high-temperature region and charge-ordered insulating state in the low-temperature region, and leads to the following consequences: (i) suppression of Jahn–Teller distortions and favors significantly ferromagnetic correlations in paramagnetic phase, resulting in significant rise of magnetization in the vicinity of T_T, (ii) simultaneously enhances the DE ferromagnetic interactions considerably in the FM domains and reduces electron-phonon coupling, (iii) P induced insulator to metallic transition at 1.02 GPa, (iv) application of P upto 2.84 GPa results in a negative giant piezoresistance of 98%, (v) no deviation in structural phase transition is observed implying by retention of hysteresis under P, (vi) a *switching-like* behavior is observed under pressure.

Acknowledgments

The authors acknowledge the DST (SERB, FIST, PURSE), BRNS, DRDO, CEFIPRA and UGC (SAP, RFSMS) for their financial support. The author R.T. acknowledges for the support of NSAF (Grant no.: U1530402). The authors wish to thank Dr. R. Mahendiran, NUS, Singapore for providing the good quality polycrystalline samples for the present work, and Prof. R. Suryanarayanan, University of Paris, France for fruitful discussions.

References

[1] (a) Y. Tokura, Rep. Prog. Phys. 69 (2006) 797;
(b) R. von Helmolt, J. Wecker, B. Holzapfel, L. Schultz, K. Samwer, Phys. Rev. Lett. 71 (1993) 2331;
(c) E.L. Nagaev, Phys. Rep. 346 (2001) 387;

(d) S. Jin, T.H. Tiefel, M. McCormack, R.A. Fastnacht, R. Ramesh, L.H. Chen, Science 264 (1994) 413.
[2] (a) E. Dagotto, T. Hotta, A. Moreo, Phys. Rep. 344 (2001) 1;
(b) C. Zenner, Phys. Rev. 83 (1951) 440;
(c) M.B. Salamon, M. Jaime, Rev. Mod. Phys. 73 (2001) 583.
[3] A.J. Millis, B.I. Shraiman, R. Mueller, Phys. Rev. Lett. **77** (1996) 175.
[4] (a) M. Jaime, M.B. Salamon, M. Rubinstein, R.E. Treece, J.S. Horwitz, D. B. Chrisey, Phys. Rev. B 54 (1996) 11914;
(b) L. Wang, J. Yin, S.Y. Huang, X.F. Hunag, J. Xu, Z.G. Liu, K.J. Chen, Phys. Rev. B 60 (1999) R6976.
[5] (a) J.J. Neumeier, M.F. Hundley, J.D. Thompson, R.H. Heffner, Phys. Rev. B 52 (1995) R7006;
(b) Z. Arnold, K. Kamenev, M.R. Ibarra, P.A. Algarabel, C. Marquina, J. Blasco, J. Garcia, Appl. Phys. Lett. 67 (1995) 2875;
(c) Y. Morimoto, A. Asamitsu, Y. Tokura, Phys. Rev. B 51 (1995) R16491;
(d) Y. Moritomo, H. Kuwahara, Y. Tokura, Phys. B 237 (1997) 26;
(e) Y. Tokura, Y. Tomioka, J. Magn. Magn. Mater. 200 (1999) 1;
(f) I.V. Medvedeva, Yu. S. Bersenev, K. Birner, L. Haupt, R. Mandal, A. Poddar, Phys. B 229 (1997) 194;
(g) V. Markovich, I. Fita, A.I. Shames, R. Puzniak, E. Rozenberg, C. Martin, A. Wisniewski, Y. Yuzhelevskii, A. Wahl, G. Gorodetsky, Phys. Rev. B 68 (2003) 094428;
(h) D.A. Mota, A. Almeida, V.H. Rodrigues, M.M.R. Costa, P. Tavares, P. Bouvier, M. Guennou, J. Kreisel, J. Agostinho Moreira, Phys. Rev. B 90 (2014) 054104 (References therein).
[6] N. Zhang, W.P. Ding, Z.B. Guo, W. Zhong, D.Y. Xing, Y.W. Du, G. Li, Y. Zheng, Z. Phys. B 102 (1997) 461.
[7] D. Mohan Radheep, P. Sarkar, S. Arumugam, P. Mandal, Appl. Phys. Lett. 102 (2013) 092406.
[8] (a) Y. Tomioka, A. Asamitsu, Y. Moritomo, Y. Tokura, J. Phys. Soc. Jpn. 64 (1995) 3626;
(b) Y. Tokura, Y. Tomioka, H. Kuwahara, A. Asamitsu, Y. Moritomo, M. Kasai, J. Appl. Phys. 79 (1996) 5288.
[9] (a) M. Bejar, R. Dharhi, F. El Haloauni, E. Dharhi, J. Alloy. Compd. 414 (2006) 31;
(b) L. Lima Sharma, P.A. Sharma, S.K. McCall, S.-B. Kim, S.-W. Cheong, Appl. Phys. Lett. 95 (2009) 092506;
(c) V.S. Kolat, T. Izgi, A.O. Kaya, N. Bayri, H. Gencer, S. Atalay, J. Magn. Magn. Mater. 322 (2010) 427;
(d) H. Sakai, Y. Taguchi, Y. Tokura, J. Phys. Soc. Jpn. 78 (2009) 113708;
(e) P. Sarkar, P. Mandal, P. Choudhuri, Appl. Phys. Lett. 92 (2008) 182506;
(f) M. Patra, S. Majumdar, S. Giri, G.N. Illes, T. Chatterji, J. Appl. Phys. 107 (2010) 076101;
(g) L. Jia, G.J. Liu, J.Z. Wang, J.R. Sun, H.W. Zhang, B.G. Shen, Appl. Phys. Lett. 89 (2006) 122515.
[10] C. Martin, A. Maignan, M. Hervieu, C. Autret, B. Raveau, D.I. Khomskii, Phys. Rev. B 63 (2001) 174402 (references therein).
[11] B. Raveau, A. Maignan, C. Martin, R. Mahendiran, M. Hervieu, J. Solid State Chem. 151 (2000) 330.
[12] A. Machida, Y. Moritomo, K. Ohoyama, T. Katsufuji, A. Nakamura, Phys. Rev. B 65 (2002) 064435.
[13] (a) H. Kuwahara, Y. Tomioka, A. Asamitsu, Y. Moritomo, Y. Tokura, Science 270 (1995) 961;
(b) M. Tokunaga, N. Miura, Y. Tomioka, Y. Tokura, Phys. Rev. B 57 (1998) 5259.
[14] (a) Congwu Cui, Trevor A. Tyson, Zhong Zhong, Jeremy P. Carlo, Yuhai Qin, Phys. Rev. B 67 (2003) 104107;
(b) Congwu Cui, Trevor A. Tysona, Appl. Phys. Lett. 83 (2003) 2856.
[15] Y. Tomioka, Y. Tokura, Phys. Rev. B 66 (2002) 104416.
[16] Y. Tomioka, A. Asamitsu, Y. Moritomo, Y. Tokura, J. Phys. Soc. Jpn. 65 (1995) 3626.
[17] V. Suresh Kumar, R. Mahendiran, J. Appl. Phys. 109 (2011) 023903.
[18] Congwu Cui, Trevor A. Tyson, Phys. Rev. B 70 (2004) 094409.
[19] (a) D.P. Kozlenko, V.I. Voronin, V.P. Glazkov, I.V. Medvedeva, B.N. Savenko, Phys. Solid State 46 (2004) 484;
(b) D.P. Kozlenko, V.P. Glazkov, Z. Jirak, B.N. Savenko, J. Magn. Magn. Mater. 267 (2003) 120.
[20] Y. Uwatoko, T. Hotta, E. Matsuoka, H. Mori, T. Ohki, J.L. Sarraot, J.D. Thompsont, N. Mori, G. Oomi, Rev. High Press Sci. Technol. 7 (1998) 1508.
[21] N. Mori, H. Takahashi, N. Takahashita, High. Press Res. 24 (2004) 225.
[22] S.W. Biernacki, Phys. Rev. B 68 (2003) 174417.
[23] C. Martin, A. Maignan, F. Damay, M. Hervieu, B. Raveau, Z. Jirak, G. André, F. Bourée, J. Magn. Magn. Mater. 202 (1999) 11.
[24] N.F. Mott, E.A. Davis, Electronic Process Ill Non-Crytalline Materials, Clarendon Press, Oxford, 1979.
[25] P. Sarkar, P. Mandal, K. Mydeen, A.K. Bera, S.M. Yusuf, S. Arumugam, C.Q. Jin, T. Ishida, S. Noguchi, Phys. Rev. B 79 (2009) 144431.
[26] S. Arumugam, Barnali Ghosh, A.K. Raychaudhuri, N.R. Tamil Selvan, T. Nakanishi, H. Yoshino, K. Murata, Ya. M. Mukovskii, J. Appl. Phys. 106 (2009) 023905.
[27] B. Lorenz, A.K. Heilman, Y.S. Wang, Y.Y. Xue, C.W. Chu, Phys. Rev. B 63 (2001) 144405.
[28] A.G. Gamzatov, A.B. Batdalov, I.K. Kamilov, Phys. B 406 (2011) 2231.
[29] M.A. Gusmao, L. Ghivelder, R.S. Freitas, R.A. Ribeiro, O.F. de Lima, F. Damay, L. F. Cohen, Solid State Commun. 127 (2003) 683.
[30] P.G. Radaelli, G. Iannone, M. Marezio, H.Y. Hwang, S.-W. Cheong, J.D. Jorgensen, D.N. Argyriou, Phys. Rev. B 56 (1997) 8265.